Int J Thermophys (2016) 37:39
DOI 10.1007/s10765-016-2049-x

ICPPP 18

Photocarrier Radiometry Investigation of Light-Induced Degradation of Boron-Doped Czochralski-Grown Silicon Without Surface Passivation

Qian Wang[1,2] · **Bincheng Li**[1,3]

Received: 7 September 2015 / Accepted: 7 February 2016 / Published online: 20 February 2016

Abstract Light-induced degradation (LID) effects of boron-doped Cz silicon wafers without surface passivation are investigated in details by photocarrier radiometry (PCR). The resistivity of all samples is in the range of 0.006 Ω·cm to 38 Ω·cm. It is found that light-induced changes in surface state occupation have a great effect on LID under illumination. With the increasing contribution of light-induced changes in surface state occupation, the generation rate of the defect decreases. The light-induced changes in surface state occupation and light-induced degradation dominate the temporal behaviors of the excess carrier density of high- and low-resistivity Si wafers, respectively. Moreover, the temporal behaviors of PCR signals of these samples under laser illumination with different powers, energy of photons, and multiple illuminations were also analyzed to understand the light-induced change of material properties. Based on the nonlinear dependence of PCR signal on the excitation power, a theoretical model taking into account both light-induced changes in surface state occupation and LID processes was proposed to explain those temporal behaviors.

Keywords B–O defect · Light-induced degradation · Photocarrier radiometry · Silicon · Surface state

This article is part of the selected papers presented at the 18th International Conference on Photoacoustic and Photothermal Phenomena.

✉ Bincheng Li
bcli@ioe.ac.cn

1 Institute of Optics and Electronics, Chinese Academy of Sciences, P. O. Box 350, Shuangliu, Chengdu 610209, China

2 University of the Chinese Academy of Sciences, Beijing 100039, China

3 School of Optoelectronic Information, University of Electronic Science and Technology of China, Chengdu 610054, China

1 Introduction

Boron (B)-doped Czochralski-grown silicon (Cz Si) suffers from a strong degradation of the minority carrier lifetime due to the formation of highly recombination-active boron–oxygen (B–O) defects under carrier injection, especially during light illumination. This phenomenon is commonly called the light-induced degradation (LID). It is a serious problem to be solved in fabricating photo-sensors and solar cell devices, and has been extensively investigated in the past [1–7]. There are two B–O defects labeled fast-stage centre (FRC) and slow-stage centre (SRC) corresponding to a fast and a slow stages of degradation, respectively. Even though the kinetics of LID effect has been extensively studied, including chemical composition [1,2], energy level [3], formation mechanism [1–6], and suppression [7] of defects, the nature of B–O defects still remains unclear up to now. In general, with good surface passivation, the effect of surface recombination on LID is neglected. However, for samples with poor or no surface passivation, the effect of the light-induced changes in surface state occupation on LID should be considered. Two electronic surface state occupations would be changed under light illumination, that is, intrinsic dangling-band and lattice-disorder surface states, which result in the decrease of the surface recombination velocity [8,9]. In the present work, LID effects of B-doped Cz Silicon wafers without surface passivation are investigated in details by photocarrier radiometry (PCR) [10,11], which is a purely carrier density-wave diagnostic method for noncontact characterization of semiconductor materials with high signal-noise ratio (SNR).

2 Materials and Experiment

The experimental PCR setup is schematically shown in Fig. 1. Three intensity-modulated super-bandgap semiconductor lasers were used as the excitation source emitting at wavelength 405 nm (3.06 eV), 660 nm (1.88 eV), and 830 nm (1.49 eV), respectively. The excitation laser beam was focused onto the sample surface to produce free carriers, and the radii of all three excitation beams at the sample surface were measured by the knife-edge method to be approximately 25 μm. The laser power was gradually varied from 1 mW to 23 mW for all samples with a variable neutral-density filter set. The photoluminescence of the photo-generated carriers, that is, the PCR signal, was collected by a pair of off-axis paraboloidal reflectors and detected by an InP/InGaAs photomultiplier (NIR PMT Module H10330A, Hamamatsu) with a spectral response range of 0.95 μm to 1.7 μm. The output signal was demodulated by a lock-in amplifier (LIA, Model 7280, Signal Recovery) and then processed by a personal computer. The PCR amplitude was recorded at room temperature as a function of the illumination time with a fixed modulation frequency of 0.8 kHz.

All samples used in this work were prepared from the batch of 4-inch p-type B-doped Cz Si wafers, with a polished front surface and a matte rear surface. They were divided into two groups by their resistivity values, as shown in Table 1. Group one were (111) oriented wafers (525 ± 25 μm thickness) with low resistivity of 0.006 Ω·cm to 0.0075 Ω·cm (S1) and 0.01 Ω·cm to 0.015 Ω·cm (S2). Group two were (100) oriented wafers (525 ± 20 μm thickness) with high resistivity of 7 Ω·cm to 13 Ω·cm (S3) and

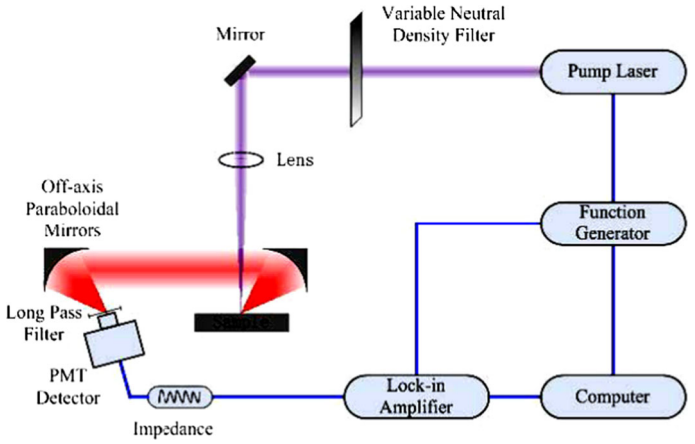

Fig. 1 Schematic diagram of PCR experimental setup

Table 1 List of samples and corresponding fitted values of β

Sample	Resistivity (Ω·cm)	Thickness (μm)	Fitted β
SR	0.012 to 0.018	550 ± 20	1.00
S1	0.006 to 0.0075	525 ± 25	1.00
S2	0.01 to 0.015	525 ± 25	1.06
S3	7 to 13	525 ± 20	1.75
S4	22 to 38	525 ± 20	1.84

22 Ω·cm to 38 Ω·cm (S4). For comparison, a (111)-oriented wafer (550 ± 20 μm thickness) with antimony (Sb) doping with resistivity of 0.012 Ω·cm to 0.018 Ω·cm (SR) was also employed. The interstitial oxygen concentrations were 13 ± 5 ppma for all samples. The change of excess minority carrier density during laser illumination was measured by means of the contactless PCR technique.

3 Theoretical Model

Similar to the rate-equation model proposed by Rodriguez et al. [8], a theoretical model taking into account both light-induced changes in surface state occupation and LID is proposed here. In this model, the change of the total excess minority carrier density (Δn) is assumed to be the result of simultaneous light-induced changes in surface state occupation and LID, in the form of

$$\Delta n\,(t) = \Delta n_0 + \Delta n_a\,(t) + \Delta n_g\,(t)\,. \tag{1}$$

Here Δn_0 is the free carrier density at the beginning of illumination. $\Delta n_a(t)$ and $\Delta n_g(t)$ are the change of free carrier density due to light-induced changes in surface state occupation and LID effects, respectively. Each surface state occupation event liberates one trapped carrier and each defect generation event traps one carrier.

Since both intrinsic dangling-bond and lattice-disorder surface states occupation [8,9] are changed, while LID process is composed of a fast and a slow recombination centre [2,3], $\Delta n_a(t)$ and $\Delta n_g(t)$ are given by

$$\Delta n_a\,(t) = N_a\,(t) = N_{a0} - N_{a1}\exp\left(-\frac{t}{\tau_{a1}}\right) - N_{a2}\exp\left(-\frac{t}{\tau_{a2}}\right), \tag{2}$$

$$\Delta n_g\,(t) = -N_g\,(t) = -N_{g0} + N_{gf}\exp\left(-\frac{t}{\tau_{gf}}\right) + N_{gs}\exp\left(-\frac{t}{\tau_{gs}}\right). \tag{3}$$

Here N_{a0} and N_{g0} are the changed surface state density and generated defect density once the steady state is reached ($t \to \infty$), respectively. $\tau_{a1,2}$ and $N_{a1,2}$ represent the characteristic trap lifetime and the densities of the surface traps, and the subscripts 1 and 2 denote intrinsic dangling-bond and lattice-disorder surface states, respectively. $\tau_{gf,s}$ and $N_{gf,s}$ represent the characteristic generation lifetime and the densities of B–O defects, and the subscripts f and s denote FRC and SRC, respectively.

To better understand the effects of light-induced changes in surface state occupation and LID on the excess minority carrier density, Fig. 2 shows the calculated excess carrier density as a function of the illumination time via Eqs. 1–3. During laser illumination, if LID is dominated, that is, $\Delta n_a \ll \Delta n_g$, and assume $\tau_{gf} = 100$ s, $\tau_{gs} = 1000$ s, $N_{gf} = N_{gs} = 0.5$, $N_{g0} = 1$, and $\Delta n_0 = 1$, more free carrier are trapped in LID resulting in the decrease of the excess minority carrier density with time. However, if light-induced changes in surface state occupation are comparable to LID, that is, $\Delta n_a \approx \Delta n_g$, and the characteristic trap lifetime is smaller than the characteristic generation lifetime, and assume $\tau_{a1} = 100$ s, $\tau_{gs} = 1000$ s, $N_{a2} = N_{gf} = 0$, $N_{a1} = N_{gs} = 0.5$, $N_{g0} = N_{a0} = 1$, and $\Delta n_0 = 1$, excess minority carrier density increases quickly first due to light-induced changes in surface state occupation, and then decreases slowly due to LID. On the other hand, if light-induced changes in surface state occupation are dominated, that is, $\Delta n_a \gg \Delta n_g$, and assume $\tau_{a1} = 100$ s, $\tau_{a2} = 1000$ s, $N_{a1} = N_{a2} = 0.5$, $N_{a0} = 1$, and $\Delta n_0 = 1$, more trapped free carrier

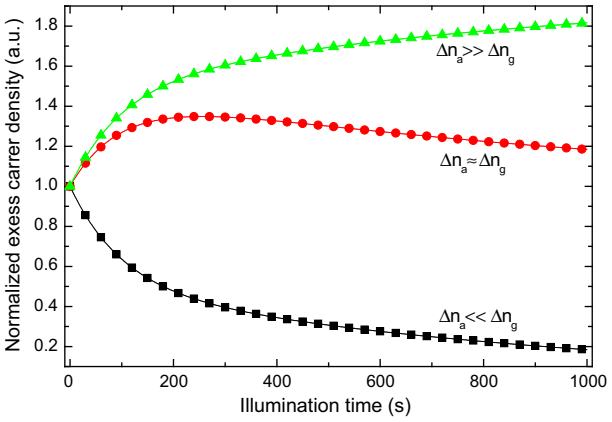

Fig. 2 Calculated normalized excess carrier density as a function of illumination time via Eqs. 1–3

are released in surface state laser annealing process resulting in the increase of excess minority carrier density with time.

The influence of electronic transport properties (the carrier lifetime, the carrier diffusion coefficient, and the front surface recombination velocity) of silicon wafers on PCR signal has been investigated in Ref. [11]. Light-induced degradation results in the reduction of the minority carrier lifetime, and light-induced changes in surface state occupation result in the reduction of the front surface recombination velocity, both of which result in the change of the minority carrier concentration as well as the PCR signal. PCR is therefore applied to investigate the LID effect in boron-doped silicon. To fit the experimental transients obtained from the p-Si samples with the proposed theoretical model, it is necessary to investigate the dependence of PCR signal on the optical excitation power. Experimental results have indicated that the dependence is nonlinear. Since the excess minority carrier density Δn is linearly proportional to the excitation power P_0, the PCR amplitude can be expressed as [12]

$$|S_{PCR}| = a P_0^{\beta} = b\Delta n^{\beta}. \tag{4}$$

Here a and b are constants, and the nonlinearity coefficient β can be given by the slope

$$\beta = \frac{\Delta \ln |S_{PCR}|}{\Delta \ln (P_0)}. \tag{5}$$

On the other hand, from the measured PCR signal, the excess minority carrier density can be extracted as

$$\Delta n = \left(|S_{PCR}| / b\right)^{1/\beta}. \tag{6}$$

4 Experimental Results and Discussion

The experimental excitation power dependences of the PCR amplitudes are measured and the results are shown in Fig. 3a. The excitation power is adjusted in the range of 1 mW to 23 mW. From these dependences, the nonlinearity coefficient for each sample is determined and the results are presented in Fig. 3b. It is clear that the β value increases with the increasing resistivity, that is, with the decreasing doping concentration. As shown in Table 1, the average β value is found to be $\sim$1.80 for group one (samples S1 and S2), while $\sim$1.03 for group two (samples S3 and S4). PCR signal is usually expressed as $\int_0^L B_{rad} \cdot (N_D + \Delta n\,(r, z))\,\Delta n\,(r, z)\,dz$ as described in Ref. [13], where B_{rad} is the coefficient of radiative recombination and N_{D} is the doping density. For low-resistivity samples S1 and S2, the excess minority carrier density $\Delta n \ll N_{\mathrm{D}}$ ($\sim 10^{19}$ cm^{-3}), PCR signal exhibits approximately linear dependence on excitation power. For high- resistivity samples S3 and S4, on the other hand, the excess minority carrier density Δn is comparable to N_{D} ($\sim 10^{16}$ cm^{-3}), and PCR signal exhibits nonlinear dependence on excitation power, as shown in Fig. 3b.

In order to monitor directly the excess minority carrier density and fit the experimental PCR data to the model proposed in Sect. 3, in the following analysis, we

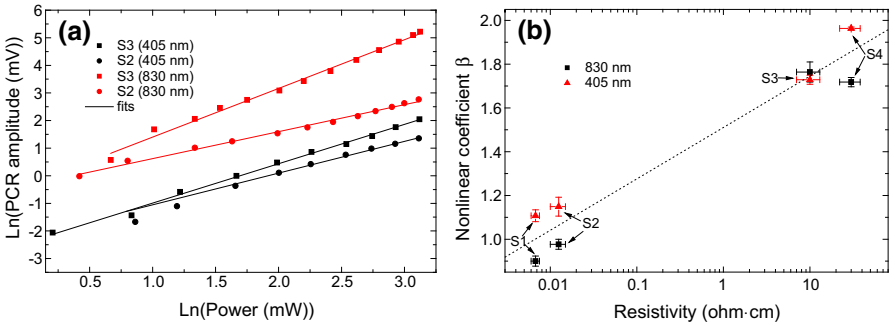

Fig. 3 (a) Ln-Ln plot of PCR amplitude versus excitation power at 405 nm and 830 nm for samples S2 and S3. (b) The extracted nonlinearity coefficient versus resistivity for samples S1–S4

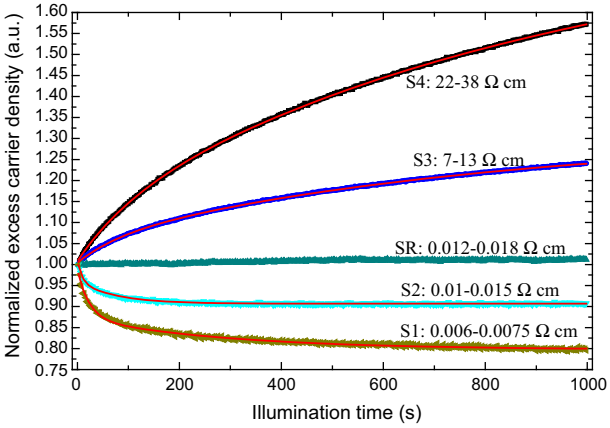

Fig. 4 Evolutions of the measured normalized excess carrier density of low- (S1, S2) and high-resistivity (S3, S4) B-doped Cz Si simples and reference sample under 830 nm laser illumination at power ∼22 mW. The β values for samples S1–S4 are 1.00, 1.06, 1.75, and 1.84, respectively

translate the PCR amplitude to the excess minority carrier density via Eq. 5 and use the β values listed in Table 1.

Figure 4 shows the experimental temporal dependence of the excess minority carrier density (normalized) under laser illumination as well as the corresponding best-fits to Eqs. 1–3 for low- (S1, S2) and high-resistivity (S3, S4) B-doped Cz Si samples. For comparison, PCR amplitude of the reference sample with Sb doping is also presented in Fig. 4. From the results of sample S2 and SR with approximate doped concentration, it is deduced that the decrease of the excess minority carrier density is related to doping boron. And, as light-induced B–O defects are widely presented in B-doped Cz Si with light illumination, this decrease is most likely related to these defects, which is the main cause resulting in degraded solar cell performance. Since the concentration N_t and generation rate $R_{gen} \equiv 1/\tau_g$ of the B–O defects increase linearly and approximately quadratic with the equilibrium and total hole concentration [2,5], respectively, the high-resistivity samples have relatively small N_t and R_{gen}, which result in negligible

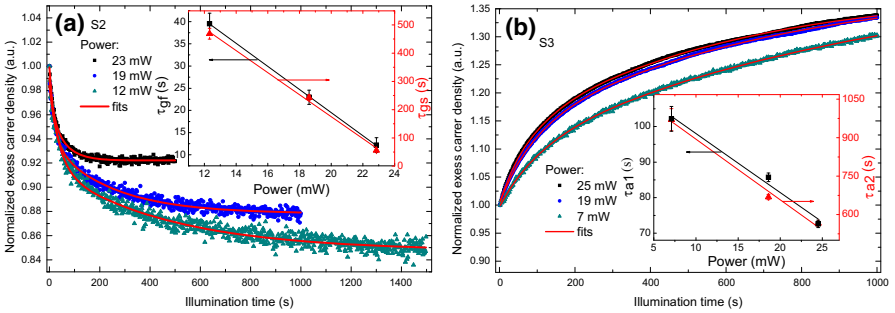

Fig. 5 Temporal evolutions of the measured normalized excess carrier density for samples S2 (a) and S3 (b) under 830 nm laser illumination at different excitation powers. *Insets* are the measured time constants as function of excitation power, showing linear response

effect on the temporal PCR signal. The excess minority carrier density increases as light-induced changes in surface state occupation dominate the temporal PCR signal. On the contrary, as low-resistivity sample has large N_t and R_{gen}, most excess minority carriers are trapped in LID, which results in the decreased excess minority carrier density. As theory predicted and experiment demonstrated, the temporal behavior of PCR of B-doped Cz Si samples is due to simultaneous light-induced changes in surface state occupation and LID effects.

Figure 5a, b show the normalized temporal evolution of the excess minority carrier density at different excitation powers at 1.49 eV (830 nm) for samples S2 and S3, respectively. The excess minority carrier density increases and the generation and trap time constants decrease with the increasing excitation power for both samples, shown in the insets of Fig. 5a, b. For sample S2, an approximately linear relationship between the generation time constant and the excitation power is found. These results are in apparent contradiction with previous studies [1] which have reported that the dependence of defect generation rate on illumination intensity saturates at values greater than 1 mW·cm^{-2}. However, Hamer et al. [5] have also observed that the increased light intensity greatly enhances the rate of defect generation, without increasing the saturation concentration of the defect. Those results suggest that the defect generation rate may depend on the excess hole concentration. Similar behavior is also observed for sample S3, as shown in Fig. 5b, indicating that impurity or defect surface states occupation is changed due to the presence of excess minority carrier.

Figure 6 shows the normalized time-dependent excess minority carrier density under laser illumination at different energy of photons for sample S2 and S3. The excitation power is approximately 22 mW for any energy of photons. Due to more injected carriers are deposited in the vicinity of surface at short excitation wavelength, the effect of surface recombination on the PCR signal is enhanced, and thus the initial excess minority carrier density decreases with the energy of photons (not shown). For sample S2, when the excitation energy of photons is small ($<$1.88 eV), the excess minority carrier density decreases gradually under laser illumination and the decay is faster with lower energy of photons. Interestingly, when the excitation energy of photons is 3.06 eV, the temporal behavior reverses with the increasing excess minority

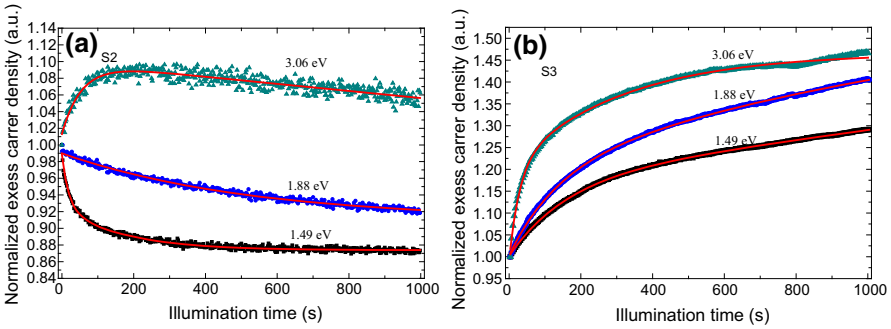

Fig. 6 Evolutions of the measured normalized excess carrier density for samples S2 (a) and S3 (b) at excitation power of $\sim$ 22 mW, at photo energies 1.49 eV, 1.88 eV, and 3.06 eV, respectively

carrier density at the first 200 s illumination. From the simulated results shown in Fig. 2, this phenomenon is related to the increasing contribution of light-induced changes in surface state occupation to the total PCR signal and the decreasing contribution of LID effect, which can be confirmed by the results of sample S3, shown in Fig. 6b. As the energy of photons increases, the rates of impurity or defect surface state occupation increase. For crystalline silicon, the optical penetration depths (defined as the reciprocal of the absorption coefficient) decrease approximately from 13.2 μm to 0.082 μm when the energy of photons increases from 1.49 eV to 3.06 eV, the excess minority carriers generated with a high energy of photons excitation are close to the surface of the sample, which results in the increasing contribution of light-induced changes in surface state occupation and the decreasing contribution of LID effect. These results indicate that the rate of surface states occupation and the rate of B–O defect generation are dependent of the energy of photons due to the depth profiles of the photoexcited carrier density.

In order to analyze the influence of multiple illuminations on the temporal behavior, circles of laser illumination at 830 nm are performed for samples S2 and S3, and the results are shown in Fig. 7. The excess minority carrier density reaches a saturation level after approximately 500 s and 3500 s illumination for samples S2 and S3, respectively. For sample S2, of considerable interest is the drop of the excess minority carrier density at the beginning of following illumination after stopping illumination for a certain time period. This phenomenon can be explained by the increase of front surface recombination velocity due to the reversibility of surface state occupation when the illumination is stopped. The reversibility of surface state occupation can be confirmed by the results of sample S3, shown in Fig. 7b. More significant decrease is observed for sample S3, due to that the illumination induced surface state occupation would be reversed when illumination stopped. This phenomenon was also found in the unpassivated n-type Si sample by photothermal radiometry (PTR) and was attributed to the reversible surface state annealing process [8]. In addition, the insets of Fig. 7a, b show that the measured excess carrier density drop Δ is approximately an exponential function of the beam off (stop illumination) period. It should be noticed that, for both high- and low-resistivity samples, no matter how long the illumination is stopped, the drop of the excess minority carrier density can quickly recover when

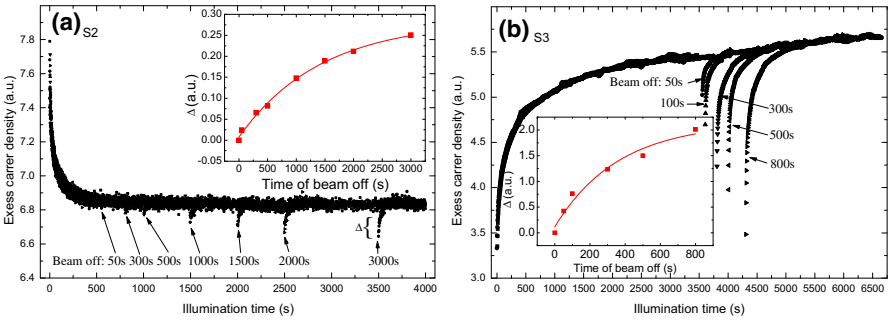

Fig. 7 Evolutions of the measured excess carrier density for sample S2 (a) and S3 (b) under circle of 830 nm laser illumination at power ∼22 mW. *Insets* are the measured excess carrier density drop Δ as function of beam off (stop illumination) period showing approximately exponential response

illumination re-starts, as shown in Fig. 7. This finding may suggest that all reversed surface state occupation is changed again in the following illumination. To conclude, it is the reversibility of surface state occupation which is responsible for the drop of the excess minority carrier density when the illumination is stopped.

5 Conclusions

In summary, we have employed PCR to investigate the light-induced degradation of boron-doped Cz Si without surface passivation. The results have shown that light-induced changes in surface state occupation have a great effect on LID under laser illumination, and light-induced changes in surface state occupation and LID effect dominated the temporal behaviors of high- and low-resistivity boron-doped Cz Si samples, respectively. Moreover, the investigation on the temporal behaviors of the excess minority carrier density of these samples under laser illumination with different powers, energy of photons, and multiple illuminations provided deeper understanding of light-induced change of material properties. PCR can be an alternative method toward the study of light-induced degradation in Cz Si through directly monitoring the excess minority carrier density and the electronic transport properties in semiconductor materials.

Acknowledgments The authors are grateful for the financial support from the National Science Foundation of China (Contract No. 61076090).

References

1. J. Schmidt, K. Bothe, Phys. Rev. B **69**, 024107 (2004)
2. K. Bothe, J. Schmidt, J. Appl. Phys. **99**, 013701 (2006)
3. V.V. Voronkov, R. Falster, J. Appl. Phys. **107**, 053509 (2010)
4. V.V. Voronkov, R. Falster, K. Bothe, B. Lim, J. Schmidt, J. Appl. Phys. **110**, 063515 (2011)
5. P. Hamer, B. Hallam, M. Abbott, S. Wenham, Phys. Status Solidi **9**(5), 297–300 (2015)
6. Y.C. Wu, X.G. Yu, P. Chen, X.Z. Chen, D.R. Yang, Appl. Phys. Lett. **104**, 102108 (2014)
7. Y.C. Wu, X.G. Yu, H. He, P. Chen, D.R. Yang, Appl. Phys. Lett. **106**, 102105 (2015)

8. M.E. Rodriguze, J.A. Garcia, A. Mandelis, C. Jean, Y. Riopel, Appl. Phys. Lett. **74**, 2429 (1999)
9. J. Opsal, M.W. Taylor, W.L. Smith, A. Rosencwaig, J. Appl. Phys. **61**, 240 (1987)
10. A. Mandelis, J. Batista, D. Shaughnessy, Phys. Rev. B **67**, 205208 (2003)
11. B. Li, D. Shaughnessy, A. Mandelis, J. Appl. Phys. **97**, 023701 (2005)
12. J. Tolev, A. Mandelis, M. Pawlak, J. Electrochem. Soc. **154**, H983 (2007)
13. J. Giesecke, *Quantitative Recombination and Transport Properties in Silicon from Dynamic Luminescence* (Springer, Freiburg, 2014)